Available online at www.sciencedirect.com
ScienceDirect
Journal of Photochemistry and Photobiology A: Chemistry 197 (2008) 18–24
Journal of Photochemistry and Photobiology A:Chemistry
www.elsevier.com/locate/jphotochem

Excited states interaction of polycyclic aromatic hydrocarbons with diphenyliodonium chloride The effective one electron reduction potential of diphenyliodonium cation

María L. Gómez [1], Hernán A. Montejano, Carlos M. Previtali *

Departamento de Química, Universidad Nacional de Río Cuarto, 5800 Río Cuarto, Argentina

Received 14 September 2007; received in revised form 26 November 2007; accepted 30 November 2007
Available online 15 December 2007

Abstract

The interaction of diphenyliodonium (DPI) cation with the excited singlet and triplet states of polycyclic aromatic hydrocarbons (PAHs) was investigated in acetonitrile solution. The kinetics of quenching was determined by time resolved experiments and the triplet and radical ions quantum yields were measured by laser flash photolysis. In the case of PAHs with short singlet lifetime (<10 ns) the singlet quenching is not an important process due to the limited solubility of DPI chloride in acetonitrile. On the other hand, for those with excited singlet lifetimes of tens of nanoseconds or longer, the singlet quenching becomes significant. However, in these cases an important decay route of the radical ion pair is intersystem crossing to the triplet state. For the triplet quenching reaction, the charge separation process is highly efficient with near 100% of the quenching events leading to radicals. Singlet and quenching rate constants fall on the same correlation with the reaction driving force. The experimental data can be fitted to a Rehm–Weller mechanism with normal parameters when a value of −0.7 V versus SCE is used for the reduction potential of DPI.

Keywords: Polycyclic aromatic hydrocarbons; Excited states; Diphenyliodonium; Electron transfer

1. Introduction

Diaryliodonium salts have been used for a long time in initiating systems for cationic [1–5] and vinyl [6–8] polymerization. However, their low absorption coefficient above 300 nm limits their use in practical systems. The spectral response of these photoinitiating systems may be extended into the 300–400 nm region by the incorporation of sensitizers. Sensitization was generally carried out with polycyclic aromatic hydrocarbons (PAHs) or aromatic ketones [1,9–12]. In these systems the iodonium cation is thought to participate as an electron acceptor in a single electron transfer step in the mechanism. The participation of both singlet and triplet states of the sensitizer in these processes was postulated [13,14].

Diaryliodonium salts are also employed in photoinitiating systems operating in the visible region [15,16]. The most common photoinitiator systems in the visible for radical polymerization are composed of a dye and an amine as an electron donor. The incorporation as a third component of an onium salt to these systems, generally a diphenyliodonium (DPI) salt, enhances the polymerization rate [6–8,17–19]. In this case an electron transfer step from the semireduced dye to the onium salt was presumed to be responsible for the accelerating effect of the salt, although the presence of DPI may affect the whole mechanism by affecting the excited states properties of the sensitizer and altering local concentrations of the reactants by means of hydrophobic aggregates [20].

For cationic photopolymerization in the visible, three components systems incorporating an iodonium salt are also known [21]. Cationic polymerization of epoxides was investigated by Bi and Neckers [21]. They found that a system consisting of a xanthene dye, an aromatic amine and a diaryliodonium salt is an efficient photoinitiator. They proposed the electron transfer

* Corresponding author.
E-mail address: cprevitali@exa.unrc.edu.ar (C.M. Previtali).
[1] Present Address: Instituto de Ciencia y Tecnología de Materiales (INTEMA), Univ. Nac. de Mar del Plata, 7600 Mar del Plata, Argentina.

1010-6030/$ – see front matter © 2007 Elsevier B.V. All rights reserved.
doi:10.1016/j.jphotochem.2007.11.027

from the dye to the iodonium salt as the primary photochemical reaction.

Several papers have deal with the mechanism of active species generation when PAHs are employed as sensitizers [1,10,14,22,23]. Electron transfer from the excited PAH to the DPI cation is generally accepted as the reaction step in which active radicals are formed. However, the role of the excited singlet and triplet states is sometimes controversial. The mechanism for cationic polymerization initiated by diaryliodonium salts sensitized by anthracenes was investigated by Nelson et al. [9] and Müller and Zücker [22]. The use of decahydroacridine diones as photosensitizers for onium salt decomposition was investigated by Timpe et al. [24]. Rate constant for singlet and triplet quenching were determined. Singlet quenching rate constants were close to the diffusional limit, while those for triplet quenching were in the order of $10^8\ M^{-1}\ s^{-1}$ for diphenyl iodonium in acetonitrile–water mixture.

The photochemistry and photophysics of iodonium salts have been reviewed by DeVoe et al. [25]. The ability of diphenyl iodonium salts to act as an electron acceptor is ascribed to its low reduction potential (E_{red}). Values as low as −0.2 V versus SCE have been reported for E_{red}. With this value prediction of reactivity and possible mechanistic steps for the participation of DPI in photoinitiating systems have been previously discussed [1,11,13,26–28]. However, using −0.2 V leads to incompatible correlations of rate constants for the quenching of excited states by DPI (vide infra). In contrast, other researchers suggest a lower value for E_{red}, ca. −0.7 V [10,14,29] and even more negative [30].

In view of the importance of diaryliodonium salts for practical uses and the interest in mechanistic aspects of their action, we undertook a detailed investigation of the interaction of diphenyliodonium chloride (DPIC) with the excited singlet and triplet states of polycyclic aromatic hydrocarbons in acetonitrile solution. The kinetics of the excited states quenching was investigated by time resolved experiments and the triplet and radical ions quantum yields were determined by laser flash photolysis. The occurrence of an electron transfer process was confirmed, although the heavy atom quenching may be the most important mechanism operating in the singlet state process. The triplet quenching rate constants thermodynamic correlation confirms a value of −0.7 V for the reduction potential of DPI.

2. Experimental

PAHs were purchased from Aldrich and were used without further purification. It was checked that their photophysical properties coincided with those reported in the literature. DPIC was provided by Aldrich. Acetonitrile, HPLC grade, was from Sintorgan.

Absorption spectra were recorded using a HP8453 diode array spectrophotometer. Steady state fluorescence experiments were carried out with a Spex Fluorolog spectrofluorometer. Fluorescence lifetime measurements were done with the time correlated single photon counting technique using Edinburgh Instruments OB-900 equipment. Transient absorption spectra and triplet quenching were determined by laser flash photolysis. A Spectron SL400 Nd:YAG laser generating 355 nm laser pulses (20 mJ per pulse, ca. 18 ns FWHM) or a Laseroptics nitrogen laser (337 nm, 4 mJ per pulse, ca. 10 ns FWHM) were the excitation sources. The laser beam was defocused in order to cover all the path length (10 mm) of the analyzing beam from a 150 W Xe lamp. The experiments were performed with rectangular quartz cells with right angle geometry. The detection system comprises a PTI monochromator coupled to a Hamamatsu R666 PM tube. The signal was acquired by a digitizing scope (Hewlett-Packard 54504) where it was averaged and then transferred to a computer. All the kinetics determinations were performed at $20 \pm 1\ ^\circ C$. For the laser photolysis experiments the solutions were de-oxygenated by bubbling during 30 min with solvent saturated high purity argon. The fluorescence quenching experiments were also carried out in de-oxygenated solutions. At the quencher concentrations employed the fluorescence was quenched without changes of the spectral shape. In addition, there were not changes in the absorption spectra of the fluorophores. Thus, ground state complex formation can be disregarded.

Quantum yields of radical cations were determined relative to the triplet yield of the PAH by means of the relation $A_R/A_T = \Phi_R\varepsilon_R/\Phi_T\varepsilon_T$ where A_R is the absorbance of the radical cation determined from the decay at one of the wavelength of the absorption maxima and extrapolated to zero time (i.e. maximum yield), A_T is the initial triplet absorbance measured at one of the maxima of the T-T absorption spectrum, $\Phi_R\varepsilon_R$ and $\Phi_T\varepsilon_T$ are the product of quantum yields and extinction coefficients at the measuring wavelength of the radical cation and triplet state, respectively. The extinction coefficients were obtained from the literature for the triplet state [31] and from Ref. [32] for the radical cations. The latter were scaled with the absorption spectra in [36] when necessary.

3. Results

3.1. Singlet quenching

Upon addition of DPIC to an acetonitrile solution of the PAHs a quenching of the fluorescence is observed without changes in the spectral shape, therefore, exciplex formation may be disregarded. Bimolecular quenching rate constants for singlet quenching (k_q) were determined from fluorescence lifetime determinations according to Eq. (1)

$$\tau^{-1} = \tau_0^{-1} + {}^1k_q[\text{DPIC}] \quad (1)$$

where τ^0 and τ stand for the fluorescence lifetime in the absence and the presence of DPIC, respectively.

The rate constants are collected in Table 1. The fluorescence lifetime of the fluorophores, measured in deoxygenated acetonitrile solutions, are also shown in Table 1.

In order to obtain information on the nature of the singlet quenching process, laser flash photolysis experiments were performed by excitation of the PAHs at 337 or 355 nm. The triplet quantum yield was determined by monitoring the T-T absorption immediately after the laser pulse. In the case of long-lived singlet states it was found that the triplet yield does not fol-

Table 1
Singlet and triplet states quenching rate constants by DPIC in MeCN at 293 K

PAH	τ_0 (ns)	E_S (kJ)[a]	^1k_q (M^{-1} s^{-1})	E_T (kJ)[b]	^3k_q (M^{-1} s^{-1})
Naphthalene (1.60)[c]	86.0	384	1.1×10^{10}	255	
Anthracene (1.09)	4.3[d]	319	1.1×10^{10}	178	1.0×10^7
Pyrene (1.16)	330	321	8.6×10^9	202	5.5×10^7
1,2-Benzanthracene (1.18)	44.2	307	8.7×10^9	198	1.5×10^7
Phenanthrene (1.50)	57.2	345	8.4×10^9	257	2.9×10^8
Tetracene (0.77)	4.9[d]	254	6.9×10^9	123	
1,2,5,6-Dibenzanthracene (1.19)	32.2	303	6.7×10^9	218	7.0×10^7
Perylene (0.85)	4.2[d]	273	1.0×10^{10}	151	7.3×10^6

The estimated error is ±5 and ±10% for singlet and triplet rate constants, respectively.
[a] Excited singlet state energy from Ref. [34].
[b] Triplet energy from ref. [34].
[c] Redox potential in volts vs. SCE in acetonitrile from Ref. [33].
[d] In air equilibrated solution.

low the same quenching behavior as the fluorescence lifetime or intensity. Moreover, in the case of pyrene an augment of the T-T absorption was observed at the same time that the singlet was quenched. These results suggest the operation of triplet induction step in the quenching mechanism, probably originated in an external heavy atom effect.

Accordingly, the singlet quenching may be accounted for by the following mechanisms

$$^1\mathrm{PAH}^* \xrightarrow{k_d} \mathrm{PAH}$$

$$^1\mathrm{PAH}^* \xrightarrow{k_{isc}} {}^3\mathrm{PAH}^*$$

$$^1\mathrm{PAH}^* + \mathrm{DPIC} \xrightarrow{fk_q} {}^3\mathrm{PAH}^* + \mathrm{DPIC}$$

$$^1\mathrm{PAH}^* + \mathrm{DPIC} \xrightarrow{(1-f)k_q} \text{quenching}$$

where f stands for the fraction of the quenching events leading to the triplet state (i.e. the efficiency of the triplet induction process) and k_q is the overall quenching rate constant.

Consequently, the triplet quantum yield may be written as

$$\Phi_T = \frac{k_{isc}}{(\tau_0^1)^{-1} + k_q[\mathrm{DPIC}]} + \frac{fk_q[\mathrm{DPIC}]}{(\tau_0^1)^{-1} + k_q[\mathrm{DPIC}]} \quad (2)$$

where τ_0^1 is the excited singlet lifetime, defined as $\tau_0^1 = (k_d + k_{isc})^{-1}$, Eq. (2) may be rearranged to

$$\frac{\Phi_T}{(\Phi_T)_0}(1 + K_{SV}[\mathrm{DPIC}]) = 1 + f\frac{k_q}{k_{isc}}[\mathrm{DPIC}] \quad (3)$$

where $(\Phi_T)_0$ and Φ_T are the triplet quantum yield in the absence and in the presence of DPIC and $K_{SV} = k_q\tau_0^1$ is the slope of the Stern Volmer (SV) plots for fluorescence quenching obtained from lifetime measurements, i.e. $\tau^0/\tau = 1 + K_{SV}[\mathrm{DPIC}]$.

Two examples of the use of Eq. (3) are given in Figs. 1 and 2, together with the SV plots for triplet yield and singlet quenching.

In Fig. 1, SV plots for the quenching of pyrene are presented. It can be seen that at the same time that the singlet is quenched, the triplet yield increases, in this case the plot of $(\Phi_T)_0/\Phi_T$ is not linear with a negative slope. Nevertheless, the plot according to Eq. (3) is linear, and from the slope, the literature value of k_{isc} and

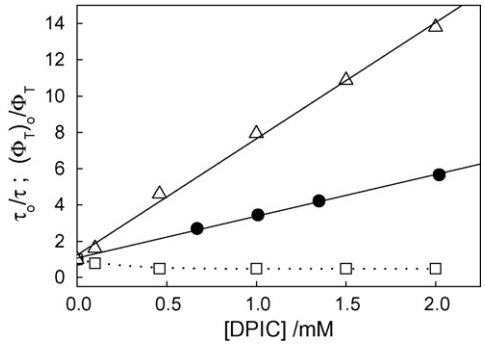

Fig. 1. Stern Volmer plots for the singlet quenching (●, τ_0/τ) and triplet yield (□, $(\Phi_T)_0/\Phi_T$) of pyrene as a function of DPIC concentration. (△) Plot of $(\Phi_T/(\Phi_T)_0)(1 + K_{SV}[\mathrm{DPIC}])$ vs. [DPIC].

the overall rate constant for singlet quenching k_q, the efficiency of triplet induction (f) may be obtained.

In Fig. 2, it is shown the SV plot for the quenching of 1,2-benzanthracene, based on measurements of the singlet lifetime, together with the similar plot for the triplet yield. It can be seen that although in this case the triplet yield decreases in the presence of the salt, the intersystem crossing is suppressed to a lesser extent than the singlet lifetime. Also in this case, a plot according to Eq. (3) is linear and from the slope the value of f could be obtained. Similar treatment for the singlet quenching and triplet yield of 1,2,5,6-dibenzanthracene and phenanthrene, the

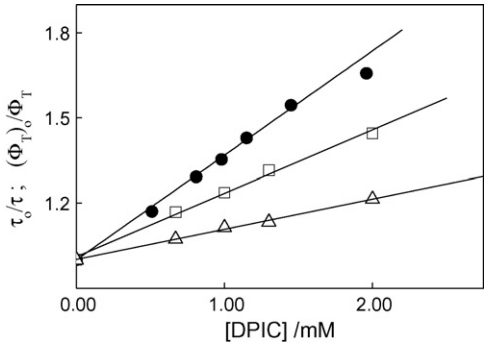

Fig. 2. Stern Volmer plots for the singlet quenching (●, τ_0/τ) and triplet yield (□, $(\Phi_T)_0/\Phi_T$) of 1,2,5,6-dibenzanthracene as a function of DPIC concentration. (△) Plot of $(\Phi_T/(\Phi_T)_0)(1 + K_{SV}[\mathrm{DPIC}])$ vs. [DPIC].

Table 2
Induced intersystem crossing efficiency in the singlet quenching by DPIC

	f	η_T [a]	k_{isc} (10^7 s^{-1})[b]
Phenanthrene	0.1 ± 0.1	0.9	1.4
1,2-Benzanthracene	0.25 ± 0.1	1.0	2.0
1,2,5,6-Dibenzanthracene	0.5 ± 0.3	0.8	3.3
Pyrene	0.9 ± 0.1	1.0	0.12

[a] Efficiency of radical formation in the triplet quenching.
[b] Intersystem crossing rate constant from triplet quantum yields and singlet lifetimes in Ref. [34].

remaining two PAHs with relatively long excited singlet lifetime, allowed also in these cases the estimation of the efficiencies of triplet induction, collected in Table 2.

Also in Table 2, the intersystem crossing rate constant of the PAHs is included. It can be seen that, with the exception of pyrene, f augments when k_{isc} increases. This result is similar to that found by Patterson and Rzad [35] for the fluorescence quenching of aromatics hydrocarbons by cesium chloride in methanol.

3.2. Triplet quenching

Triplet quenching was measured by laser flash photolysis by monitoring the decay of the T-T absorption in the presence of DPIC. Bimolecular quenching rate constants (^3k_q) were obtained from a plot of the pseudo-first order decay rate constants of the triplet state (k_{obs}) as a function of DPIC concentration, Eq. (4). The rate constants are collected in Table 1.

$$k_{obs} = k^0 + {}^3k_q[\text{DPIC}] \quad (4)$$

The transient absorption spectra at long times of the PAHs in the presence of DPIC show, in all cases, the typical bands of the radical cation of the PAH. This confirms the electron transfer nature of the quenching process. Typical spectra are shown in Figs. 3 and 4.

In Fig. 3, the transient absorption spectra of phenanthrene in the absence and the presence of DPIC 1.2 mM are presented. In the absence of the salt the spectrum presents the typical bands of the T-T absorption of phenanthrene at 425, 455 and 485 nm [31]. In the presence of DPIC the spectrum is totally different

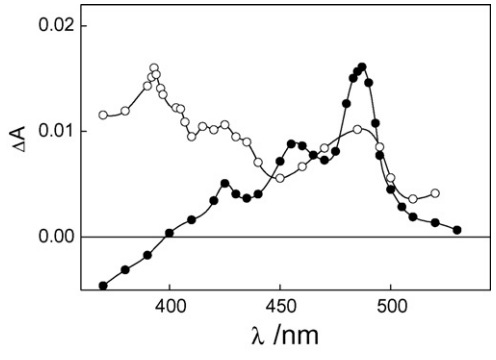

Fig. 3. Transient absorption spectrum of phenanthrene taken at 10 μs after the laser pulse in the absence (●) and the presence (◯) of DPIC 1.2 mM.

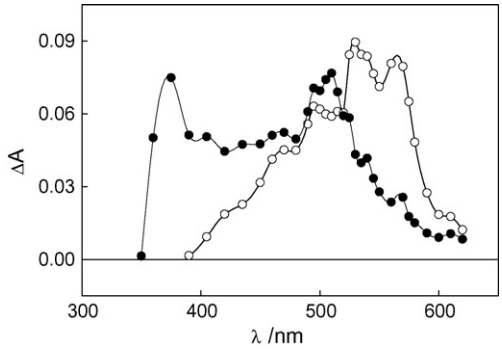

Fig. 4. Transient absorption spectrum of 1,2,5,6-dibenzanthracene in the presence of DPIC 2 mM at 1 μs (◯) and 40 μs (●) after the laser pulse.

with bands at 393, 425 and 485 nm that can be ascribed to the radical cation of phenanthrene [36].

In Fig. 4, the spectrum of 1,2,5,6-dibenzanthracene is shown in the presence of DPIC 2.0 mM at 1 μs and at 40 μs after the laser pulse. At short times the spectrum shows the bands of the T-T absorption at 495, 530 and 565 nm [31]. At longer times these bands are replaced by the absorption of the radical cation of the hydrocarbon at 375 and 510 nm [36].

Thus, the laser flash photolysis experiments substantiate an electron transfer quenching process.

$$^3\text{PAH} + \text{DPI}^+ \rightarrow \text{PAH}^{\bullet+} + \text{DPI}^\bullet$$

This is followed by a fast breakdown of $\text{DPI}^\bullet$ radical [10]

$$\text{DPI}^\bullet \rightarrow \text{PhI} + \text{Ph}^\bullet$$

It is the phenyl radical formed in the last reaction that is active in promoting polymerization.

3.3. Radicals yield

The radical quantum yield produced in the deactivation of PAHs excited states by DPIC is given by

$$\Phi_{rad} = \Phi * \beta\eta \quad (5)$$

where Φ^* stands for the quantum yield of excited state formation in the presence of DPIC, β is the fraction of excited states quenched, and η is the fraction of these events that leads to active radicals. Since radical ions can be produced from the singlet and triplet excited states of the PAHs with DPIC, the total radical quantum yield is given by

$$\Phi_{rad} = (\Phi_{rad})_S + (\Phi_{rad})_T \quad (6)$$

Each term in Eq. (6) may be written in the form of Eq. (5) with β given by Eq. (7)

$$\beta = \frac{k_q[\text{DPIC}]}{k_q[\text{DPIC}] + \sum k^0} \quad (7)$$

where k_q is the respective quenching rate constant and $\sum k^0 = \tau_0^{-1}$ is the sum of all the first order decays of the excited state. In this way the maximum ($\eta = 1$) radical quantum yield can be

calculated from the measured values of the quenching rate constants, the excited state lifetimes, and the triplet quantum yield, as given in Eq. (8)

$$\Phi_{\text{rad}} = \frac{\eta_S {}^1k_q[\text{DPIC}]}{{}^1k_q[\text{DPIC}] + (\tau_0^1)^{-1}} + \frac{\eta_T \Phi_T {}^3k_q[\text{DPIC}]}{{}^3k_q[\text{DPIC}] + (\tau_0^3)^{-1}} \quad (8)$$

The triplet quantum yield to be used in the second term in Eq. (8) has to be corrected by the singlet quenched by DPIC and the efficiency of the triplet induction process, as given by Eq. (2). At low quencher concentration the fraction of excited singlet states quenched would be low. Moreover, as explained above, the majority of the singlet quenching events lead to the triplet state. Therefore, the first term in Eq. (8) may be disregarded. In this way, by comparison of the theoretical maximum radical yield with the experimental value, determined as explained in the experimental section, η_T can be estimated. The results are collected in Table 2. They are affected by a considerable error, which is difficult to evaluate, due mainly to the uncertainty in the absorption coefficient of the radicals and triplet state. Nevertheless, the values given in Table 2 point consistently to an efficiency close to unity for the triplet process.

4. Discussion

As can be seen in Table 1, both singlet and quenching rate constants vary with the oxidation potential of the PAH according to a charge transfer process. This is further corroborated by the presence of the radical ions as manifested by the transient spectra. Although in the singlet quenching reaction the main product is the triplet state, the trend in the rate constant is also consistent with the intermediacy of a geminate radical ions pair (RIP). Therefore, a correlation of the rate constants with the Gibbs energy change for the overall electron transfer process, ΔG°, is expected. The latter may be calculated from the redox potentials of the donor $E_{(D/D^+)}$ and acceptor $E_{(A/A^-)}$, and the energy E^* of the excited state involved, with the Rehm–Weller equation [37]

$$\Delta G^\circ = E_{(D/D^+)} - E_{(A/A^-)} - E* + C \quad (9)$$

where C is the coulombic energy term.

The excited states energies and redox potential of the PAHs are well-established quantities (Table 1). This is not the case for the reduction potential of DPI. As discussed above, values in the range −0.2 to −0.7 V versus SCE can be found in different sources. If the first value is adopted, ΔG° will be negative even for the less reactive process, the triplet quenching of perylene, for which −0.52 eV results when −0.2 V is used for E_{red}. However, the value of the rate constant measured for this process, $7.3 \times 10^6\ M^{-1}\ s^{-1}$ (Table 1) is incompatible with this exergonicity for a single electron transfer reaction. The triplet quenching rate constants in Table 1 are in line with a more negative value for the reduction potential of DPI. This is further corroborated by comparison with other well-characterized electron transfer quenching of triplet states by electron acceptors. Thus, the triplet state quenching of PAHs by nitrobenzenes, with potentials from −1.02 to −0.86 V, presents

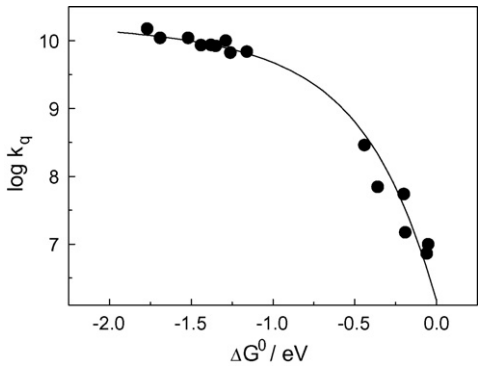

Fig. 5. Singlet and triplet quenching rate constants as a function of the free energy change.

rate constants varying from 9×10^5 to $2.4 \times 10^7\ M^{-1}\ s^{-1}$ for anthracene and from 5×10^8 to $6 \times 10^9\ M^{-1}\ s^{-1}$ for 1,2,5,6-dibenzanthracene in acetonitrile [38]. These values are similar, or even higher than those for the quenching by DPIC in Table 1. Moreover, alkyl substituted *p*-benzoquinones have one electron reduction potential in the range of −0.5 to −0.84 V and they quench the triplet state of the dye safranine with rate constants in the range of 3×10^7–$3 \times 10^9\ M^{-1}\ s^{-1}$ in methanol and 4×10^6–$4 \times 10^8\ M^{-1}\ s^{-1}$ in acetonitrile [39]. For the same dye we measured in aqueous solution a quenching rate constant by DPIC of $1 \times 10^6\ M^{-1}\ s^{-1}$ [19]. In summary, by comparison of the triplet quenching rate constants of different electron acceptors with the values in Table 1, it can be concluded that a reasonable value for the reduction potential of DPIC in acetonitrile should be ca. −0.7 V as measured by other researches [10,14,29] and not −0.2 V as repeatedly employed for discussing the reactivity of the salt in electron transfer processes.

In order to confirm the reasonability of this figure, we tried a free energy correlation using −0.7 V for E_{red}. In Fig. 5, the quenching rate constants for the singlet and triplet quenching in acetonitrile are plotted versus ΔG° with the latter calculated with Eq. (9) with a value of −0.7 V for $E_{(A/A^-)}$. The Rehm–Weller mechanism for electron transfer quenching was adopted, Scheme 1, where D^* and Q stands for the excited PAH and the quencher, respectively.

The steady state quenching rate constant is

$$k_q = \frac{k_{12}}{1 + ((k_{21}/k_{23})((k_{32}/k_{30}) + 1))} \quad (10)$$

introducing the Gibbs energy change for the electron transfer process,

$$\frac{k_{23}}{k_{32}} = \exp\left(\frac{-\Delta G^*}{RT}\right) \quad (11)$$

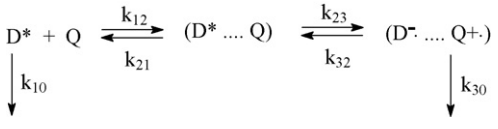

Scheme 1.

and

$$k_{23} = k_{23}^{0} \exp\left(\frac{-\Delta G^{*}}{\mathrm{RT}}\right) \quad (12)$$

Eq. (10) becomes

$$k_{q} = \frac{k_{12}}{1 + (k_{21}/k_{23}^{0})\exp(\Delta G^{*}/\mathrm{RT}) + (k_{21}/k_{30})\exp(\Delta G^{\circ}/\mathrm{RT})} \quad (13)$$

After introduction of reasonable assumptions for the kinetics parameters, Eq. (13) may be simplified to [37]

$$k_{q} = \frac{k_{12}}{1 + 0.25[\exp(\Delta G^{*}/\mathrm{RT}) + \exp(\Delta G^{\circ}/\mathrm{RT})]} \quad (14)$$

with

$$\Delta G^{*} = \frac{\Delta G^{\circ}}{2} + \left[\left(\frac{\Delta G^{\circ}}{2}\right)^{2} + [\Delta G^{*}(0)]^{2}\right]^{1/2} \quad (15)$$

where $\Delta G^{*}(0)$ is the activation free energy change for $\Delta G^{\circ} = 0$ and it is an adjustable parameter. The solid line in Fig. 5 is drawn using Eqs. (9)–(15) with $3.1 \times 10^{10}\ \mathrm{M^{-1}\ s^{-1}}$ for k_{12} and 0.3 eV for $\Delta G^{*}(0)$. These parameters are in line with those found in several kinetics correlations for electron transfer processes in acetonitrile. This, together with the goodness of the fitting may be taken as a confirmation that the DPIC redox potential is ca. −0.7 V or even more negative, but not the value of −0.2 V.

It can be seen that both singlet and triplet quenching fall on the same correlation. The main difference for singlet and triplet quenching resides in the last step k_{30}. In the case of singlet quenching it involves three different pathways of decay of the geminate radical pair, the back electron transfer to ground state, the cage escape of the radicals and dissociation of the DPI radical, and intersystem crossing to the triplet state of the PAH. The latter being favored by the heavy atom effect of the iodine atom in DPI. Meanwhile, for the triplet state as seen by the high yield of radical ions, the most important decay route is the escape of the radicals.

5. Conclusions

The excited states quenching of PAHs takes place by an electron transfer mechanism. In the case of PAHs with short singlet lifetime (<10 ns) the singlet quenching is not an important process due to the limited solubility of DPIC in acetonitrile. Otherwise, for those with lifetimes of tens of nanoseconds or longer, the singlet quenching becomes significant. However, in these cases an important decay route of the radical ion pair is intersystem crossing to the triplet state. Differently, for the triplet quenching reaction, the charge separation process is highly efficient with near 100% of the quenching events leading to radicals. Singlet and triplet quenching rate constants fall on the same correlation with the reaction driving force. The experimental data can be fitted to a Rehm–Weller mechanism with normal parameters when a value of −0.7 V is used for the reduction potential of DPI. If a value of −0.2 V is used instead the data cannot be adjusted to the model with reasonable values for the rest of the parameters.

Acknowledgments

Thanks are given to Consejo Nacional de Investigaciones Científicas y Técnicas (CONICET – PIP 5605), Agencia Nacional de Promoción Científica (ANPCYT – PICTO 30244/05) and Universidad Nacional de Río Cuarto, Argentina, for financial support of this work.

References

[1] S.P. Pappas, L.R. Gatechair, J.H. Jilek, J. Polym. Sci. A: Polym. Chem. 22 (1984) 77.
[2] G. Manivannan, J.P. Fouassier, J.V. Crivello, J. Polym. Sci. A: Polym. Chem. 30 (1992) 1999.
[3] Y. Yagci, I. Reetz, Prog. Polym. Sci. 23 (1998) 1485.
[4] Y. Yagci, Y. Hepuzer, Macromolecules 32 (1999) 6367.
[5] Y. Toba, J. Photopolym. Sci. Technol. 16 (2003) 115.
[6] A. Erddalane, J.P. Fouassier, F. Morlet-Savary, Y. Takimoto, J. Polym. Sci. A: Polym. Chem. 34 (1996) 633.
[7] K.S. Padon, A.B. Scranton, J. Polym. Sci. A: Polym. Chem. 38 (2000) 2057.
[8] D. Kim, A. Scranton, J. Polym. Sci. A: Polym. Chem. 42 (2004) 5863.
[9] E.W. Nelson, T.P. Carter, A.B. Scranton, J. Polym. Sci. A: Polym. Chem. 33 (1995) 247.
[10] A. Kunze, U. Müller, K. Tittes, J.P. Fouassier, F. Morlet-Savary, J. Photochem. Photobiol. A: Chem. 110 (1997) 115.
[11] J.V. Crivello, M. Sangermano, J. Polym. Sci. A: Polym. Chem. 39 (2001) 343.
[12] H.J. Timpe, A.G. Rajendran, Eur. Polym. J. 27 (1991) 77.
[13] C. Selvaraju, A. Sivakumar, P. Ramamurthy, J. Photochem. Photobiol. A: Chem. 138 (2001) 213.
[14] A.C. Bruce, J.J. Klein, M.R.V. Sahyun, J. Photochem. Photobiol. A: Chem. 131 (2000) 27.
[15] Q.Q. Zhu, W. Schnabel, Polymer 37 (1996) 4129.
[16] J.P. Fouassier, X. Allonas, D. Burget, Prog. Org. Coatings 47 (2003) 16.
[17] K.S. Padon, A.B. Scranton, J Polym Sci A: Polym. Chem. 39 (2001) 715.
[18] C. Grotzinger, D. Burget, P. Jacques, J.P. Fouassier, Polymer 44 (2003) 3671.
[19] M.L. Gómez, V. Avila, H.A. Montejano, C.M. Previtali, Polymer 44 (2003) 2875.
[20] M.L. Gómez, H.A. Montejano, M. Bohorquez, C.M. Previtali, J. Polym. Sci. A: Polym. Chem. 42 (2004) 4916.
[21] Y. Bi, D.C. Neckers, Macromolecules 27 (1994) 3683.
[22] U. Müller, I. Zücker, J. Photochem. Photobiol. A: Chem. 120 (1999) 93.
[23] Y. Toba, M. Saito, Y. Usui, Macromolecules 32 (1999) 3209.
[24] H.J. Timpe, S. Ulrich, J.P. Fouassier, J. Photochem. Photobiol. A: Chem. 73 (1993) 139.
[25] R.J. DeVoe, P.M. Olofson, M.R.V. Sahyun, Adv. Photochem. 17 (1992) 313.
[26] H. Braun, Y. Yagci, O. Nuyken, Eur. Polym. J. 38 (2002) 151.
[27] C. Dursun, M. Degirmenci, Y. Yagci, S. Jockusch, N.J. Turro, Polymer 44 (2003) 7389.
[28] Y. He, W. Zhou, F. Wu, M. Li, E. Wang, J. Photochem. Photobiol. A: Chem. 162 (2004) 463.
[29] R.J. Devoe, M.R. Sahyun, N. Serpone, D.K. Sharma, Can. J. Chem. 65 (1987) 2342.
[30] S. Fung, S.C. Moratti, S.C. Graham, R.H. Friend, Synth. Metals 102 (1999) 1167.
[31] I. Carmichael, G.L. Hug, J. Phys. Chem. Ref. Data 15 (1986) 1.
[32] C. Sato, K. Kikuchi, K. Okamura, Y. Takahashi, T. Miyashi, J. Phys. Chem. 99 (1995) 16925.
[33] A.J. Baird, H. Lund (Eds.), Encyclopedia of the Electrochemistry of the Elements. Organic Section, vol XI, Marcel Dekker, New York, 1984.
[34] S.L. Murov, I. Carmichael, G.L. Hug, Handbook of Photochemistry, 2nd Ed., Marcel Dekker, NY, 1993.

[35] L.K. Patterson, S.J. Rzad, Chem. Phys. Lett. 31 (1975) 254.
[36] T. Shida, Electronic Spectra of Radical Ions, Elsevier, Amsterdam, 1988.
[37] D. Rehm, A. Weller, Ber. Bunsen-Ges. Phys. Chem. 73 (1969) 834; D. Rehm, A. Weller, Isr. J. Chem. 8 (1970) 259.
[38] H.A. Montejano, V. Avila, H.A. Garrera, C.M. Previtali, J. Photochem. Photobiol. A 72 (1993) 117.
[39] S.G. Bertolotti, C.M. Previtali, J. Photochem. Photobiol. A 103 (1997) 115.